

Measurement of Leading Particle Effects in Decays of Z^0 Bosons into Light Flavors*

The SLD Collaboration**

Stanford Linear Accelerator Center, Stanford University, Stanford, CA 94309

Abstract

We present evidence for leading particle production in hadronic decays of the Z^0 boson to light-flavor jets. A polarized electron beam was used to tag quark and antiquark jets, and a vertex detector was employed to reject heavy-flavor events. Charged hadrons were identified with a Cherenkov ring imaging detector. In the quark jets, more high-momentum p , Λ , K^- , and \bar{K}^{*0} were observed than their antiparticles, and vice versa for antiquark jets, providing direct evidence that the higher-momentum particles in jets are more likely to carry the primary quark or antiquark from the Z^0 decay, and that $s\bar{s}$ production is suppressed in fragmentation.

Submitted to Physical Review Letters

*Work supported by Department of Energy contracts: DE-FG02- 91ER40676 (BU), DE-FG03-91ER40618 (UCSB), DE-FG03- 92ER40689 (UCSC), DE-FG03- 93ER40788 (CSU), DE-FG02- 91ER40672 (Colorado), DE-FG02- 91ER40677 (Illinois), DE-AC03- 76SF00098 (LBL), DE-FG02- 92ER40715 (Massachusetts), DE-FC02- 94ER40818 (MIT), DE-FG03- 96ER40969 (Oregon), DE-AC03- 76SF00515 (SLAC), DE-FG05- 91ER40627 (Tennessee), DE-FG02- 95ER40896 (Wisconsin), DE-FG02- 92ER40704 (Yale); National Science Foundation grants: PHY-91- 13428 (UCSC), PHY-89- 21320 (Columbia), PHY-92- 04239 (Cincinnati), PHY-95- 10439 (Rutgers), PHY-88- 19316 (Vanderbilt), PHY-92- 03212 (Washington); The UK Particle Physics and Astronomy Research Council (Brunel and RAL); The Istituto Nazionale di Fisica Nucleare of Italy (Bologna, Ferrara, Frascati, Pisa, Padova, Perugia); The Japan-US Cooperative Research Project on High Energy Physics (Nagoya, Tohoku); The Korea Science and Engineering Foundation (Soongsil).

A fundamental issue in strong-interaction jet fragmentation is that of the transport of quantum numbers of primary interacting partons into the observed final-state particles. In non-diffractive hadron-hadron collisions, final-state particles with large values of the longitudinal beam momentum fraction x_F have been observed that contain one or more valence quarks of the same type as those in one or both of the initial-state particles. This has been interpreted in terms of an initial-state quark participating in the collision and being carried in a particular “leading” final-state particle that tends to have a large fraction of the energy of the resulting jet [1]. In $e^+e^- \rightarrow c\bar{c}$ ($b\bar{b}$) events, D (B) hadrons have been found [2] to carry a large fraction of the beam energy and to be produced at a rate of approximately two per $c\bar{c}$ or $b\bar{b}$ event, indicating that these hadrons are produced predominantly as leading particles.

Such leading particle production in jet fragmentation is predicted by several iterative models of the hadronization process [3]. However, the extent to which this effect is present in light-flavor jets (u , \bar{u} , d , \bar{d} , s , or \bar{s}) in e^+e^- interactions has not been studied experimentally because of difficulties involved with tagging jets initiated by a specific light flavor and with separating quark jets from antiquark jets. If such a separation were achieved, a signature for the leading particle effect in a sample of quark jets would be an excess of a hadron species containing the isolated valence quark type over its antiparticle, and vice versa for antiquark jets. One could then study the momentum distributions, flavors and spin states of leading hadrons and antihadrons in each such flavor sample.

If one could separate samples of light quark (u , d , s) and antiquark (\bar{u} , \bar{d} , \bar{s}) jets, then a leading particle effect might appear as an excess in the quark sample of baryons over antibaryons, since the valence constituents of baryons are quarks rather than antiquarks. Also, the cross sections for $e^+e^- \rightarrow u\bar{u}$ and $e^+e^- \rightarrow d\bar{d}$ or $s\bar{s}$ are not in general equal, so a signal in quark jets for leading production of charged mesons, such as π^- and K^- , might be visible. Furthermore, one might observe an excess of a meson over its antimeson if it is produced more often in jets initiated by one valence flavor rather than the other. For example, a suppression of $s\bar{s}$ relative to $u\bar{u}$ and $d\bar{d}$ production in the fragmentation process might cause more leading K^- (\bar{K}^{*0}) to be produced in s jets than in \bar{u} (\bar{d}) jets.

In this letter we present the first study of leading particle production in light flavor jets in e^+e^- annihilation, using 150,000 hadronic Z^0 decay events produced by the SLAC Linear Collider (SLC) and recorded in the SLC Large Detector (SLD) from 1993 to 1995. We define a particle to be leading if it carries a primary quark or antiquark, namely the q or \bar{q} in $e^+e^- \rightarrow Z^0 \rightarrow q\bar{q}$, where $q = u, d$, or s . We separated jets initiated by primary quarks from those initiated by primary antiquarks by utilizing the electroweak forward-backward production asymmetry in the polar angle, enhanced by the high SLC electron beam polarization. We suppressed the large background from heavy-flavor ($Z^0 \rightarrow c\bar{c}$ or $b\bar{b}$) events, in which the decay products of a heavy hadron can exhibit a leading particle effect, by using information from the Vertex Detector (VXD) [4]. The Cherenkov Ring Imaging Detector (CRID) [5] was used to identify charged hadrons. We measured the production rates of π^- , K^- , \bar{K}^{*0} , p , and Λ as a function of momentum in light-quark jets and compared them with the rates of their respective antiparticles. We interpret the observed differences in terms of leading particles.

A description of the detector, trigger, track and hadronic event selection, and Monte Carlo simulation is given in Ref. [6]. Cuts were applied in order to select events well-contained within the detector acceptance, resulting in a sample of approximately 90,000 events. Heavy-flavor events often include tracks associated with separated decay points of short-lived heavy hadrons, and were suppressed by requiring all tracks passing a set of quality cuts to extrapolate to within three standard deviations from the interaction point in the plane transverse to the beam. The selected sample was estimated from our Monte Carlo simulation to consist of 85% light-flavor events, with residual backgrounds of 12% $c\bar{c}$ and 3% $b\bar{b}$ events.

Z^0 bosons decay predominantly into a left-handed quark and a right-handed antiquark. In $e^+e^- \rightarrow Z^0 \rightarrow q\bar{q}$ events, when the electron beam has longitudinal polarization P_e , the quark prefers to follow the electron (positron) beam direction for left-(right-) handed e^- beam, and its polar angle θ with respect to the electron beam is distributed as $(1 + \cos^2 \theta + 2A_q A_Z \cos \theta)$, where $A_Z = (A_e - P_e)/(1 - A_e P_e)$, and A_e and A_q are the asymmetry parameters for electrons and quarks respectively. In the Standard Model $A_e = 0.16$, $A_u = A_c = 0.67$ and $A_d = A_s = A_b = 0.94$. For this analysis we considered all events to consist of one jet in each of the two hemispheres separated by the plane perpendicular to the thrust axis [7], and required the thrust axis polar angle θ_t to satisfy $|\cos \theta_t| > 0.2$. Defining the forward direction to be along the electron beam, the quark jet was defined to comprise the set of tracks in the forward (backward) hemisphere for events recorded with left-(right-) handed electron beam. The opposite jet in each event was defined to be the antiquark jet. For roughly two-thirds of the sample, $|P_e| = 0.77$ [8], for the remainder $|P_e| = 0.63$ [9], and there were equal numbers of left- and right-handed beam pulses. For these conditions, the Standard Model at tree level predicts the purities of the quark- and antiquark-tagged samples to be about 73%.

We then measured the production rates per light quark jet

$$R_h^q = \frac{1}{2N_{evts}} \frac{d}{dx_p} [N(q \rightarrow h) + N(\bar{q} \rightarrow \bar{h})], \quad (1)$$

$$R_{\bar{h}}^q = \frac{1}{2N_{evts}} \frac{d}{dx_p} [N(q \rightarrow \bar{h}) + N(\bar{q} \rightarrow h)], \quad (2)$$

where: q and \bar{q} represent light-flavor quark and antiquark jets respectively; N_{evts} is the total number of events in the sample; h represents any of the identified hadrons π^- , K^- , \bar{K}^{*0} , p , and Λ , and \bar{h} indicates the corresponding antiparticle; x_p is the scaled momentum $2p/\sqrt{s}$ of the hadron, where p is its magnitude of momentum and \sqrt{s} is the e^+e^- center-of-mass energy. Then, for example, $N(q \rightarrow h)$ is the number of hadrons of type h in light quark jets.

The identification of π^\pm , K^\pm , p , and \bar{p} was achieved by reconstructing emission angles of individual Cherenkov photons radiated by charged particles passing through liquid and gas radiator systems of the SLD CRID. For each track, a likelihood was constructed for each of these particle hypotheses, based upon the number of detected photons and their measured angles, and the expected number of photons, Cherenkov angle, and background. Particle separation was based on the differences among the likelihoods. Identification was achieved [10, 11] over the momentum range $0.5 < p < 35 \text{ GeV}/c$.

Positively charged tracks in the quark-tagged sample and negatively charged tracks in the antiquark-tagged sample gave consistent results and were combined into one sample. In

each x_p bin, identified π , K , and p were counted, and these counts were unfolded using the inverse of the identification efficiency matrix \mathbf{E} [10, 11], and corrected for track reconstruction efficiency to yield values of $R_{\pi^+}^q$, $R_{K^+}^q$, and R_p^q in the tagged samples. The same procedure applied to the remaining tracks yielded $R_{\pi^-}^q$, $R_{K^-}^q$, and $R_{\bar{p}}^q$. The elements E_{ij} , denoting the momentum-dependent probability to identify a true i -type particle as a j -type particle, were measured from the data for $i = \pi, p$ and $j = \pi, K, p$ using tracks from selected K_S^0 , τ and Λ decays. A detailed Monte Carlo simulation was used to derive the remaining elements in terms of these measured ones.

Candidate $\Lambda \rightarrow p\pi^-$ and $\bar{\Lambda} \rightarrow \bar{p}\pi^+$ decays were selected by considering all pairs of oppositely charged tracks that were inconsistent with originating at the interaction point and passed a set of cuts [12] on vertex quality and flight distance. Backgrounds from K_S^0 decays and photon conversions were suppressed by using kinematic cuts. Candidate $K^{*0} \rightarrow K^+\pi^-$ and $\bar{K}^{*0} \rightarrow K^-\pi^+$ decays were selected by considering all pairs of oppositely-charged tracks if one track was identified in the CRID as a charged kaon, the other was not so identified, and the tracks were consistent with intersecting at the interaction point [13].

The Λ candidates in quark-tagged jets and the $\bar{\Lambda}$ candidates in antiquark-tagged jets were assigned to one sample, and the remaining $\Lambda/\bar{\Lambda}$ candidates to a second sample. In each x_p bin, the number of observed $\Lambda/\bar{\Lambda}$ in each sample was determined from a fit to the $p\pi$ invariant mass distribution. These signals were corrected for reconstruction efficiency to yield R_{Λ}^q and $R_{\bar{\Lambda}}^q$ in the tagged samples. The \bar{K}^{*0} and K^{*0} candidates were similarly divided into two samples, and the $K\pi$ invariant mass distributions were fitted to obtain $R_{K^{*0}}^q$ and $R_{\bar{K}^{*0}}^q$.

In every x_p bin, each measured R_h^q and $R_{\bar{h}}^q$ was further corrected for the contribution from residual heavy-flavor events, estimated from our Monte Carlo simulation. Finally, the corrected R_h^q and $R_{\bar{h}}^q$ were unfolded for the purity of the quark jet tag.

These production rates are shown in Figure 1. There are no K^\pm or p/\bar{p} points in the range $0.12 < x_p < 0.20$ due to the lack of CRID particle separation in this region. Systematic errors arising from the uncertainties in the backgrounds in the identified particle samples, in the measured electron beam polarization, and in the backgrounds from heavy-flavor events were included and were found to be much smaller than the statistical errors. Not shown in the figure are uncertainties common to particles and their respective antiparticles, including those arising from track reconstruction and particle-identification efficiency. These are typically 2-5%.

We define the difference between each particle and antiparticle production rate, normalized by the sum:

$$D_h = \frac{R_h^q - R_{\bar{h}}^q}{R_h^q + R_{\bar{h}}^q},$$

for which the common systematic uncertainties cancel. As shown in Figure 2, for each hadron h , D_h is consistent with zero for $x_p < 0.1$. D_{π^-} is also consistent with zero for $x_p > 0.1$, but for the other hadrons $D_h > 0$ for $x_p \gtrsim 0.2$. The JETSET 7.4 [14] and HERWIG 5.8 [15] fragmentation models were found to reproduce these features qualitatively.

Since baryons contain no constituent antiquarks, we interpret the positive D_p and D_Λ as evidence for leading baryon production in light-flavor jets. If pions and kaons exhibited

similar leading effects, then one would expect $D_{\pi^-} \approx D_{K^-} \approx 0.27D_{baryon}$, and $D_{\bar{K}^{*0}} = 0$, assuming Standard Model quark couplings to the Z^0 . For purposes of illustration, the result of a linear fit to the D_p and D_Λ points above $x_p = 0.2$ was scaled by 0.27 and is shown in Figs. 2(c) and 2(d). The observed D_{π^-} are below this line, and are consistent with zero at all x_p , suggesting that either there is little production of leading pions, or there is substantial background from non-leading pions or pions from decays of resonances such as the ρ and K^* . For $x_p > 0.2$, we observe $D_{K^-} > 0.27D_{baryon}$ and $D_{\bar{K}^{*0}} > 0$. This indicates both substantial production of leading K and K^* mesons at high momentum, and a depletion of leading kaon production in $u\bar{u}$ and $d\bar{d}$ events relative to $s\bar{s}$ events.

Assuming these high-momentum kaons to be directly produced in the fragmentation process, this amounts to a direct observation of a suppression of $s\bar{s}$ production from the vacuum with respect to $u\bar{u}$ or $d\bar{d}$ production. In the case of K^{*0} mesons it has been suggested [16] that this effect can be used to measure the “strangeness suppression parameter” γ_s , that is an important component of models of hadronization, see e.g. Ref. [14]. Assuming *all* K^{*0} and \bar{K}^{*0} in the range $x_p > 0.5$ to be leading, we calculate $\gamma_s = 0.26 \pm 0.12$, consistent with values [17] derived from inclusive measurements of the relative production rates of strange and non-strange, pseudoscalar and vector mesons.

In summary, we have studied leading particle effects in hadronic Z^0 decays. In the light quark jets, we observed an excess of Λ over $\bar{\Lambda}$, and an excess of p over \bar{p} . These differences increase with momentum, and provide direct evidence for the “leading particle” hypothesis that faster baryons are more likely to contain the primary quark. No such difference was observed between π^- and π^+ production. For kaons, we observed a significant excess of high momentum K^- over K^+ , and \bar{K}^{*0} over K^{*0} , indicating that a fast kaon is likely to contain a primary quark or antiquark from the Z^0 decay, and that leading kaons are produced predominantly in $s\bar{s}$ events rather than $d\bar{d}$ or $u\bar{u}$ events.

We thank the personnel of the SLAC accelerator department and the technical staffs of our collaborating institutions for their outstanding efforts on our behalf.

References

- [1] For a review, see M. Basile *et al.*, *Il Nuovo Cimento A* **66** (1981) 129.
- [2] ALEPH Collab.: D. Buskulic *et al.*, *Z. Phys. C* **62** (1994) 179;
DELPHI Collab.: P. Abreu *et al.*, *Z. Phys. C* **66** (1995) 323;
L3 Collab.: B. Adeva *et al.*, *Phys. Lett. B* **261** (1991) 177;
OPAL Collab.: R. Akers *et al.*, *Z. Phys. C* **60** (1993) 199.
- [3] R.D. Field and R.P. Feynman, *Nucl. Phys. B* **136** (1978) 1;
B. Andersson *et al.*, *Phys. Rep.* **97** (1983) 33.
- [4] C.J.S. Damerell *et al.*, *Nucl. Inst. Meth.* **A288** (1990) 288.
- [5] K. Abe *et al.*, *Nucl. Inst. Meth.* **A343** (1994) 74.
- [6] SLD Collab.: K. Abe *et al.*, *Phys. Rev. D* **53** (1996) 1023.

- [7] S. Brandt *et al*, Phys. Lett. **12** (1964) 57;
E. Farhi, Phys. Rev. Lett. **39** (1977) 1587.
- [8] SLD Collab.: K. Abe *et al*, SLAC-PUB-7291 (1996), submitted to Phys. Rev. Lett.
- [9] SLD Collab.: K. Abe *et al*, Phys. Rev. Lett. **73** (1994) 25.
- [10] SLD Collab.: K. Abe *et al*, SLAC-PUB-7399 (1996), in preparation.
- [11] T.J. Pavel, Ph.D. Thesis, Stanford University, 1996, SLAC-R-491 (1996).
- [12] K.G. Baird, Ph.D. Thesis, Rutgers University, 1996, SLAC-R-483 (1996).
- [13] SLD Collab.: M. Dima *et al*, SLAC-PUB-7280 (1996), to appear in *Proceedings of the 9th Meeting of the Division of Particles and Fields of the American Physical Society*, Minneapolis, MN, Aug. 10-15, 1996.
- [14] T. Sjöstrand, Comp. Phys. Comm. **82** (1994) 74.
- [15] G. Marchesini *et al*, Comp. Phys. Comm. **67** (1992) 465.
- [16] G.D. Lafferty, Phys. Lett. B **353** (1995) 541.
- [17] D.H. Saxon, *High Energy Electron-Positron Physics*, Eds. A. Ali and P. Söding, World Scientific (1988), p. 539.

**List of Authors

K. Abe,⁽¹⁹⁾ K. Abe,⁽³⁰⁾ T. Akagi,⁽²⁸⁾ N.J. Allen,⁽⁴⁾ W.W. Ash,^{(28)†} D. Aston,⁽²⁸⁾
K.G. Baird,⁽²⁴⁾ C. Baltay,⁽³⁴⁾ H.R. Band,⁽³³⁾ M.B. Barakat,⁽³⁴⁾ G. Baranko,⁽⁹⁾
O. Bardon,⁽¹⁵⁾ T. L. Barklow,⁽²⁸⁾ G.L. Bashindzhagyan,⁽¹⁸⁾ A.O. Bazarko,⁽¹⁰⁾
R. Ben-David,⁽³⁴⁾ A.C. Benvenuti,⁽²⁾ G.M. Bilei,⁽²²⁾ D. Bisello,⁽²¹⁾ G. Blaylock,⁽¹⁶⁾
J.R. Bogart,⁽²⁸⁾ B. Bolen,⁽¹⁷⁾ T. Bolton,⁽¹⁰⁾ G.R. Bower,⁽²⁸⁾ J.E. Brau,⁽²⁰⁾
M. Breidenbach,⁽²⁸⁾ W.M. Bugg,⁽²⁹⁾ D. Burke,⁽²⁸⁾ T.H. Burnett,⁽³²⁾ P.N. Burrows,⁽¹⁵⁾
W. Busza,⁽¹⁵⁾ A. Calcaterra,⁽¹²⁾ D.O. Caldwell,⁽⁵⁾ D. Calloway,⁽²⁸⁾ B. Camanzi,⁽¹¹⁾
M. Carpinelli,⁽²³⁾ R. Cassell,⁽²⁸⁾ R. Castaldi,^{(23)(a)} A. Castro,⁽²¹⁾ M. Cavalli-Sforza,⁽⁶⁾
A. Chou,⁽²⁸⁾ E. Church,⁽³²⁾ H.O. Cohn,⁽²⁹⁾ J.A. Coller,⁽³⁾ V. Cook,⁽³²⁾ R. Cotton,⁽⁴⁾
R.F. Cowan,⁽¹⁵⁾ D.G. Coyne,⁽⁶⁾ G. Crawford,⁽²⁸⁾ A. D'Oliveira,⁽⁷⁾ C.J.S. Damerell,⁽²⁵⁾
M. Daoudi,⁽²⁸⁾ R. De Sangro,⁽¹²⁾ R. Dell'Orso,⁽²³⁾ P.J. Dervan,⁽⁴⁾ M. Dima,⁽⁸⁾
D.N. Dong,⁽¹⁵⁾ P.Y.C. Du,⁽²⁹⁾ R. Dubois,⁽²⁸⁾ B.I. Eisenstein,⁽¹³⁾ R. Elia,⁽²⁸⁾ E. Etzion,⁽³³⁾
S. Fahey,⁽⁹⁾ D. Falciari,⁽²²⁾ C. Fan,⁽⁹⁾ J.P. Fernandez,⁽⁶⁾ M.J. Fero,⁽¹⁵⁾ R. Frey,⁽²⁰⁾
K. Furuno,⁽²⁰⁾ T. Gillman,⁽²⁵⁾ G. Gladding,⁽¹³⁾ S. Gonzalez,⁽¹⁵⁾ E.L. Hart,⁽²⁹⁾ J.L. Harton,⁽⁸⁾
A. Hasan,⁽⁴⁾ Y. Hasegawa,⁽³⁰⁾ K. Hasuko,⁽³⁰⁾ S. J. Hedges,⁽³⁾ S.S. Hertzbach,⁽¹⁶⁾
M.D. Hildreth,⁽²⁸⁾ J. Huber,⁽²⁰⁾ M.E. Huffer,⁽²⁸⁾ E.W. Hughes,⁽²⁸⁾ H. Hwang,⁽²⁰⁾
Y. Iwasaki,⁽³⁰⁾ D.J. Jackson,⁽²⁵⁾ P. Jacques,⁽²⁴⁾ J. A. Jaros,⁽²⁸⁾ A.S. Johnson,⁽³⁾
J.R. Johnson,⁽³³⁾ R.A. Johnson,⁽⁷⁾ T. Junk,⁽²⁸⁾ R. Kajikawa,⁽¹⁹⁾ M. Kalelkar,⁽²⁴⁾
H. J. Kang,⁽²⁶⁾ I. Karliner,⁽¹³⁾ H. Kawahara,⁽²⁸⁾ H.W. Kendall,⁽¹⁵⁾ Y. D. Kim,⁽²⁶⁾
M.E. King,⁽²⁸⁾ R. King,⁽²⁸⁾ R.R. Kofler,⁽¹⁶⁾ N.M. Krishna,⁽⁹⁾ R.S. Kroeger,⁽¹⁷⁾ J.F. Labs,⁽²⁸⁾
M. Langston,⁽²⁰⁾ A. Lath,⁽¹⁵⁾ J.A. Lauber,⁽⁹⁾ D.W.G.S. Leith,⁽²⁸⁾ V. Lia,⁽¹⁵⁾ M.X. Liu,⁽³⁴⁾
X. Liu,⁽⁶⁾ M. Loreti,⁽²¹⁾ A. Lu,⁽⁵⁾ H.L. Lynch,⁽²⁸⁾ J. Ma,⁽³²⁾ G. Mancinelli,⁽²²⁾ S. Manly,⁽³⁴⁾
G. Mantovani,⁽²²⁾ T.W. Markiewicz,⁽²⁸⁾ T. Maruyama,⁽²⁸⁾ H. Masuda,⁽²⁸⁾ E. Mazzucato,⁽¹¹⁾
A.K. McKemey,⁽⁴⁾ B.T. Meadows,⁽⁷⁾ R. Messner,⁽²⁸⁾ P.M. Mockett,⁽³²⁾ K.C. Moffeit,⁽²⁸⁾
T.B. Moore,⁽³⁴⁾ D. Muller,⁽²⁸⁾ T. Nagamine,⁽²⁸⁾ S. Narita,⁽³⁰⁾ U. Nauenberg,⁽⁹⁾ H. Neal,⁽²⁸⁾
M. Nussbaum,⁽⁷⁾ Y. Ohnishi,⁽¹⁹⁾ D. Onoprienko,⁽²⁹⁾ L.S. Osborne,⁽¹⁵⁾ R.S. Panvini,⁽³¹⁾
C.H. Park,⁽²⁷⁾ H. Park,⁽²⁰⁾ T.J. Pavel,⁽²⁸⁾ I. Peruzzi,^{(12)(b)} M. Piccolo,⁽¹²⁾ L. Piemontese,⁽¹¹⁾
E. Pieroni,⁽²³⁾ K.T. Pitts,⁽²⁰⁾ R.J. Plano,⁽²⁴⁾ R. Prepost,⁽³³⁾ C.Y. Prescott,⁽²⁸⁾
G.D. Punkar,⁽²⁸⁾ J. Quigley,⁽¹⁵⁾ B.N. Ratcliff,⁽²⁸⁾ T.W. Reeves,⁽³¹⁾ J. Reidy,⁽¹⁷⁾
P.L. Reinertsen,⁽⁶⁾ P.E. Rensing,⁽²⁸⁾ L.S. Rochester,⁽²⁸⁾ P.C. Rowson,⁽¹⁰⁾ J.J. Russell,⁽²⁸⁾
O.H. Saxton,⁽²⁸⁾ T. Schalk,⁽⁶⁾ R.H. Schindler,⁽²⁸⁾ B.A. Schumm,⁽⁶⁾ J. Schwiening,⁽²⁸⁾
S. Sen,⁽³⁴⁾ V.V. Serbo,⁽³³⁾ M.H. Shaevitz,⁽¹⁰⁾ J.T. Shank,⁽³⁾ G. Shapiro,⁽¹⁴⁾ D.J. Sherden,⁽²⁸⁾
K.D. Shmakov,⁽²⁹⁾ C. Simopoulos,⁽²⁸⁾ N.B. Sinev,⁽²⁰⁾ S.R. Smith,⁽²⁸⁾ M.B. Smy,⁽⁸⁾
J.A. Snyder,⁽³⁴⁾ P. Stamer,⁽²⁴⁾ H. Steiner,⁽¹⁴⁾ R. Steiner,⁽¹⁾ M.G. Strauss,⁽¹⁶⁾ D. Su,⁽²⁸⁾
F. Suekane,⁽³⁰⁾ A. Sugiyama,⁽¹⁹⁾ S. Suzuki,⁽¹⁹⁾ M. Swartz,⁽²⁸⁾ A. Szumilo,⁽³²⁾
T. Takahashi,⁽²⁸⁾ F.E. Taylor,⁽¹⁵⁾ E. Torrence,⁽¹⁵⁾ A.I. Trandafir,⁽¹⁶⁾ J.D. Turk,⁽³⁴⁾
T. Usher,⁽²⁸⁾ J. Va'vra,⁽²⁸⁾ C. Vannini,⁽²³⁾ E. Vella,⁽²⁸⁾ J.P. Venuti,⁽³¹⁾ R. Verrier,⁽¹⁵⁾
P.G. Verdini,⁽²³⁾ D.L. Wagner,⁽⁹⁾ S.R. Wagner,⁽²⁸⁾ A.P. Waite,⁽²⁸⁾ S.J. Watts,⁽⁴⁾
A.W. Weidemann,⁽²⁹⁾ E.R. Weiss,⁽³²⁾ J.S. Whitaker,⁽³⁾ S.L. White,⁽²⁹⁾ F.J. Wickens,⁽²⁵⁾
D.A. Williams,⁽⁶⁾ D.C. Williams,⁽¹⁵⁾ S.H. Williams,⁽²⁸⁾ S. Willocq,⁽²⁸⁾ R.J. Wilson,⁽⁸⁾
W.J. Wisniewski,⁽²⁸⁾ M. Woods,⁽²⁸⁾ G.B. Word,⁽²⁴⁾ J. Wyss,⁽²¹⁾ R.K. Yamamoto,⁽¹⁵⁾

J.M. Yamartino,⁽¹⁵⁾ X. Yang,⁽²⁰⁾ J. Yashima,⁽³⁰⁾ S.J. Yellin,⁽⁵⁾ C.C. Young,⁽²⁸⁾ H. Yuta,⁽³⁰⁾
G. Zapalac,⁽³³⁾ R.W. Zdarko,⁽²⁸⁾ and J. Zhou,⁽²⁰⁾

⁽¹⁾ *Adelphi University, Garden City, New York 11530*

⁽²⁾ *INFN Sezione di Bologna, I-40126 Bologna, Italy*

⁽³⁾ *Boston University, Boston, Massachusetts 02215*

⁽⁴⁾ *Brunel University, Uxbridge, Middlesex UB8 3PH, United Kingdom*

⁽⁵⁾ *University of California at Santa Barbara, Santa Barbara, California 93106*

⁽⁶⁾ *University of California at Santa Cruz, Santa Cruz, California 95064*

⁽⁷⁾ *University of Cincinnati, Cincinnati, Ohio 45221*

⁽⁸⁾ *Colorado State University, Fort Collins, Colorado 80523*

⁽⁹⁾ *University of Colorado, Boulder, Colorado 80309*

⁽¹⁰⁾ *Columbia University, New York, New York 10027*

⁽¹¹⁾ *INFN Sezione di Ferrara and Università di Ferrara, I-44100 Ferrara, Italy*

⁽¹²⁾ *INFN Lab. Nazionali di Frascati, I-00044 Frascati, Italy*

⁽¹³⁾ *University of Illinois, Urbana, Illinois 61801*

⁽¹⁴⁾ *E.O. Lawrence Berkeley Laboratory, University of California, Berkeley, California
94720*

⁽¹⁵⁾ *Massachusetts Institute of Technology, Cambridge, Massachusetts 02139*

⁽¹⁶⁾ *University of Massachusetts, Amherst, Massachusetts 01003*

⁽¹⁷⁾ *University of Mississippi, University, Mississippi 38677*

⁽¹⁸⁾ *Moscow State University, Institute of Nuclear Physics 119899 Moscow, Russia*

⁽¹⁹⁾ *Nagoya University, Chikusa-ku, Nagoya 464 Japan*

⁽²⁰⁾ *University of Oregon, Eugene, Oregon 97403*

⁽²¹⁾ *INFN Sezione di Padova and Università di Padova, I-35100 Padova, Italy*

⁽²²⁾ *INFN Sezione di Perugia and Università di Perugia, I-06100 Perugia, Italy*

⁽²³⁾ *INFN Sezione di Pisa and Università di Pisa, I-56100 Pisa, Italy*

⁽²⁴⁾ *Rutgers University, Piscataway, New Jersey 08855*

⁽²⁵⁾ *Rutherford Appleton Laboratory, Chilton, Didcot, Oxon OX11 0QX United Kingdom*

⁽²⁶⁾ *Sogang University, Seoul, Korea*

⁽²⁷⁾ *Soongsil University, Seoul, Korea 156-743*

⁽²⁸⁾ *Stanford Linear Accelerator Center, Stanford University, Stanford, California 94309*

⁽²⁹⁾ *University of Tennessee, Knoxville, Tennessee 37996*

⁽³⁰⁾ *Tohoku University, Sendai 980 Japan*

⁽³¹⁾ *Vanderbilt University, Nashville, Tennessee 37235*

⁽³²⁾ *University of Washington, Seattle, Washington 98195*

⁽³³⁾ *University of Wisconsin, Madison, Wisconsin 53706*

⁽³⁴⁾ *Yale University, New Haven, Connecticut 06511*

† *Deceased*

^(a) *Also at the Università di Genova*

^(b) *Also at the Università di Perugia*

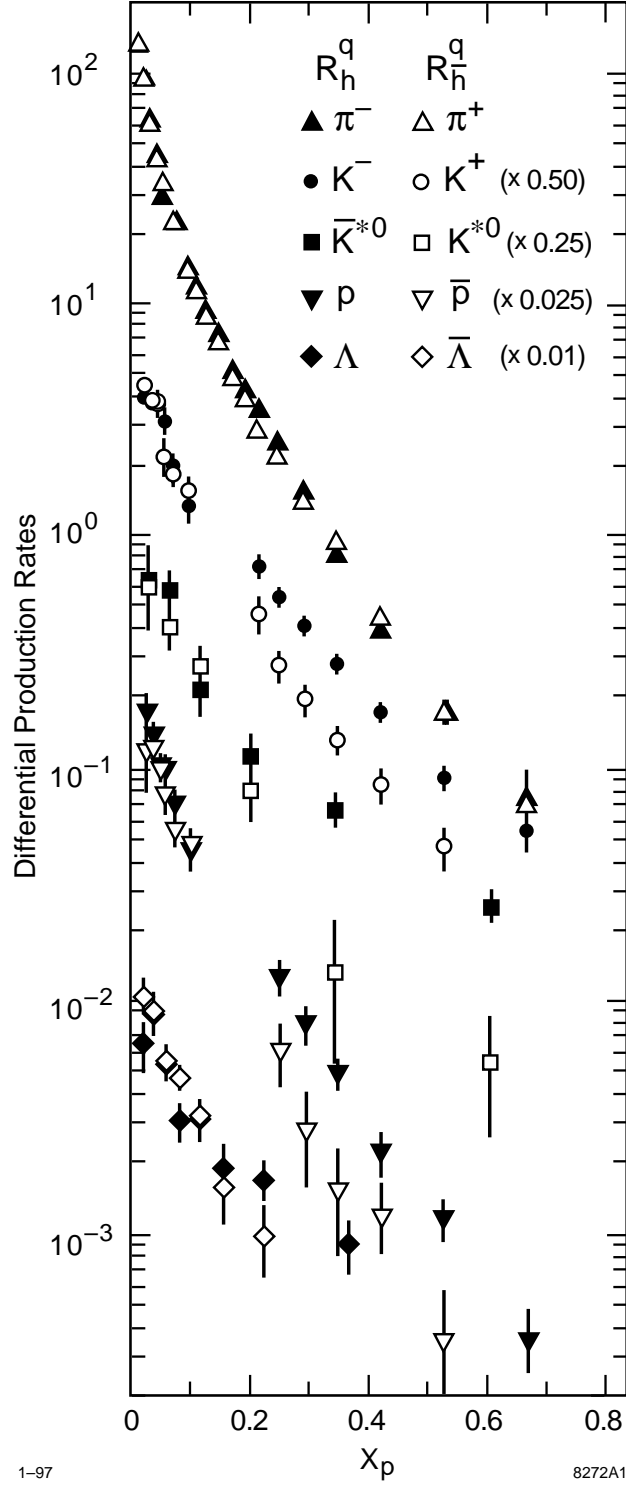


Figure 1: Differential production rates as a function of scaled momentum. The ordinates represent average multiplicities per light quark jet per unit interval in scaled momentum.

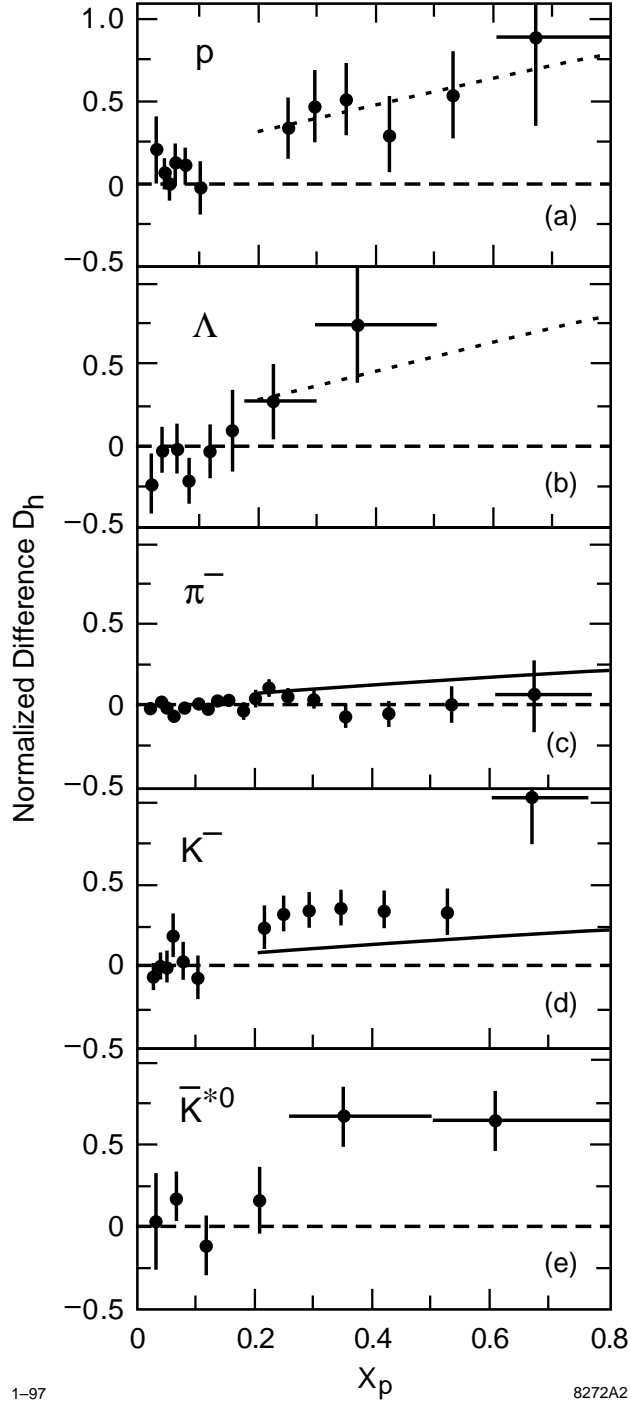


Figure 2: Normalized production differences (dots) as a function of scaled momentum. The horizontal error bars on selected points indicate their bin widths. The dotted lines represent a linear fit to the D_p and D_Λ points for $x_p > 0.2$, and the solid lines are this fit scaled by the factor 0.27 discussed in the text.